

APPLICATION OF TURBULENT DIFFUSIVITY MODELS TO POINT-SOURCE DISPERSION IN OUTDOOR AND INDOOR FLOWS

H.D. Lim

School of Civil, Aerospace and Design Engineering
University of Bristol
Bristol, BS8 1TR, United Kingdom
desmond.lim@bristol.ac.uk

Christina Vanderwel

Department of Aeronautics and Astronautics
University of Southampton
Southampton, SO16 7QF, United Kingdom
C.M.Vanderwel@soton.ac.uk

ABSTRACT

The modelling and prediction of scalar transport in turbulent flows is crucial for many environmental and industrial flows. We discuss the key findings of our experimental campaigns which focus on two relevant applications: the scalar dispersion of a ground-level point-source in (1) a smooth-wall turbulent boundary layer flow and (2) a supply-ventilated empty room model. For advection-dominated outdoor flows, we show how a Gaussian Plume Model provides a good framework to describe the mean scalar field and discuss its limitations in (wrongly) assuming a constant turbulent diffusivity. For indoor flows, we explore the balance of the advective and turbulent fluxes and their dependence on the room geometry and source position. We use our improved understanding on the scalar transport mechanism in these applications to assess the application of turbulent diffusivity models to predict scalar dispersion, highlighting the importance of carefully defining what the eddy diffusivity coefficient encompasses in different approaches.

INTRODUCTION

Hazardous air pollutants released in public spaces are a threat to national security and can have long-lasting repercussions on the public health and economy. Managing the consequences of these incidents often requires time-sensitive decisions that need to be supported by science. As such, it is important to have the capability to model the scalar dispersion of hazardous air pollutants accurately and quickly.

The transport of a scalar quantity from a continuous point-source is challenging to model in turbulent shear flows and can be approached in several ways depending on the application. In the absence of surface deposition or chemical reactions (i.e. negligible sources/sinks), the mean flow advection and turbulent diffusion are the two dominant processes that can affect the scalar transport. The Reynolds-averaged advection-diffusion equation which describes the mean concentration (\bar{C}) of a species is:

$$\frac{\partial \bar{C}}{\partial t} + \underbrace{\bar{U}_i \frac{\partial \bar{C}}{\partial x_i}}_{\text{mean advection}} + \underbrace{\frac{\partial \overline{c'u'_i}}{\partial x_i}}_{\text{eddy diffusion}} = 0. \quad (1)$$

The simplest model for dealing with the turbulent scalar fluxes, $\overline{c'u'_i}$, is the gradient transport model which is given as:

$$-\overline{c'u'_i} = D_{ij} \frac{\partial \bar{C}}{\partial x_j}, \quad (2)$$

where D_{ij} is the eddy (turbulent) diffusivity tensor, which reduces to a single coefficient ($K\delta_{ij} = D_{ij}$, where δ_{ij} is the Kronecker delta) in isotropic turbulence. There is a huge body of literature that are based on the advection-diffusion and gradient transport model framework. This includes studies on uniformly sheared flow (Vanderwel & Tavoularis, 2014), indoor room flow (van Hooff *et al.*, 2014) and wall-bounded flow (Lim & Vanderwel, 2023). More generally, steady RANS simulations which do not provide concentration and velocity fluctuations, would have to rely on the eddy diffusion coefficient as a way to calculate the turbulent scalar fluxes using the mean properties.

For outdoor environmental applications, where the flow is typically unidirectional, the advection-diffusion equation is an ideal framework for tracking air pollution. In this case, under the assumptions of steady state flow, and that the mean advection dominates the eddy diffusion in the along wind direction, the analytical solution to the advection-diffusion equation for an elevated point source is given by the reflected Gaussian plume model as:

$$\bar{C}(x, y, z) = \frac{\dot{M}}{2\pi\bar{U}\sigma_y\sigma_z} \exp\left(-\frac{z^2}{2\sigma_z^2}\right) \left[\exp\left(-\frac{(y-H)^2}{2\sigma_y^2}\right) + \exp\left(-\frac{(y+H)^2}{2\sigma_y^2}\right) \right] = 0. \quad (3)$$

In equation 3, \dot{M} represents the mass flow rate of the emission source, \bar{U} is the average wind velocity in the prevailing direction, H is the height of the source above the ground, and σ_y and σ_z are the dispersion coefficients (i.e. standard deviation of the Gaussian concentration distribution (Stockie, 2011)) corresponding to the y and z directions, which are the wall-normal and lateral coordinates (both perpendicular to the wind direction x) respectively.

Examples of Gaussian models for air quality modelling include the US-EPA model AERMOD (Cimorelli *et al.*, 2005) and the ADMS model developed by the CERC and the UK Meteorological Office (Carruthers *et al.*, 2000). Although this approach has been used heavily in outdoor air quality modelling, it relies heavily on empirical estimates of the turbulent diffusivity to control the growth of the scalar plume.

For indoor air quality modelling, the room flow is usually more complex than outdoor flows, since the mean flow patterns are dependent on the air change per hour (ACH) (Cheng *et al.*, 2011), ventilation design and the room geometry (Foat *et al.*, 2020). To avoid having to resolve the complex flow patterns or separately resolve the mean flow advection in indoor spaces, an alternative framework is commonly used in indoor airflow applications where there is a lack of dominant flow direction. In this case, the scalar dispersion problem can be modelled using the diffusion equation framework (Fick's second law), which is the same as equation 1 but without the mean advection term. Recent studies based on this approach include the experimental study on the repeated passage of a single cylinder in a channel (Mingotti *et al.*, 2020), the continuous release of carbon monoxide in indoor spaces (Cheng *et al.*, 2011) and the determination of the turbulent diffusion coefficient in a mechanically ventilated room using the turbulent kinetic energy balance (Foat *et al.*, 2020).

The analytical solution to the diffusion equation (Fick's second law) produces an Eddy Diffusion Model (Nicas *et al.*, 2009) which is favoured for short duration dispersion events in the absence of dominant mean flow advection. This is given as:

$$\bar{C}(x, y, z, t) = \frac{M \exp(-\lambda_f t)}{8(\pi K t)^{3/2} r_x r_y r_z}. \quad (4)$$

where M is the mass of pollutant released at $t=0$, λ_f is the air change rate, K is the turbulent diffusivity coefficient, and r_x , r_y and r_z are wall reflection terms, implemented as image sources to satisfy the no-flux wall boundaries (Nicas *et al.*, 2009).

This approach assumes the contribution of the mean flow advection to the scalar transport is isotropic and homogeneous at the room length-scale and is often simply described as 'negligible mean flow advection' in the Eddy Diffusion Model literature. In effect, the contribution of advective transport to the mixing of the scalar is consolidated with the turbulent transport into the total diffusivity term K . Strictly speaking, the total diffusivity term K in equation 4 is therefore, *not the same* as $K\delta_{ij} = D_{ij}$ in equation 2.

The Eddy Diffusion Model is particularly well-suited for applications where the total eddy diffusion coefficient which controls the net scalar dispersion rate is known (Cheng *et al.*, 2011; Foat *et al.*, 2020). Although it has been shown to be valid in many indoor airflow scenarios (Cheng *et al.*, 2011; Shao *et al.*, 2017; Foat *et al.*, 2020), its accuracy is reliant on selecting the right value of the total eddy diffusion coefficient which depends on the flow parameters and source location.

Regardless of the flow application, the turbulent diffusivity is an important parameter that controls the scalar transport. Although most scalar dispersion models require only a single eddy diffusion coefficient to predict the concentration of pollutants, Calder (1965) has presented theoretical proof showing the turbulent diffusivity tensor cannot be diagonal unless the flow turbulence is isotropic. In real-world applications, flow turbulence is rarely isotropic, and measurements of an anisotropic and non-homogeneous turbulent diffusivity tensor have been observed in several different flow applications (Lim & Vanderwel, 2023; Tavoularis & Corrsin, 1985).

In this paper, we examine the application of turbulent diffusivity models to two idealised turbulent flow applications representing outdoor and indoor flows, respectively: the scalar dispersion of a ground-level point-source in (1) a smooth-wall turbulent boundary layer (TBL) and (2) a supply-ventilated empty room. We discuss the uncertainties associated with approximating the experimental measurements of the turbulent diffusivity tensor to a single effective eddy diffusion coefficient (by assuming turbulence is isotropic) which is required for scalar dispersion models. We discuss the validity of each model's assumptions, for instance 'negligible mean flow advection' in Eddy Diffusion Models, and their implications on the predicted concentration under various flow conditions.

METHODOLOGY

Experiments were performed in a recirculating water tunnel using simultaneous particle-image velocimetry (PIV) and planar laser-induced fluorescence (PLIF) which allow us to measure the advective and turbulent fluxes in the flow. Figure 1 illustrates the two separate setups: (a) a point source released in a smooth-wall TBL and (b) a point source released in an enclosed room mounted upside down in the facility. Rhodamine 6G fluorescent dye (Schmidt number, $Sc=2500$) was used as a proxy for the pollutant. The dye flow rate was maintained at $Q_{dye}=10 \text{ mL min}^{-1}$ and introduced isokinetically at ground-level using an embedded 2.5 mm tube, with source concentrations (C_s) adjusted to maximise the dynamic range of the PLIF camera. Polyamide seeding particles (50 μm) were added to the flume and recirculated until the desired seeding density and uniformity were achieved. The fluorescent dye and seeding particles were illuminated with a Nd:YAG double-pulsed laser, and wavelength filters were used to separate the PIV and PLIF signals to the cameras. The PIV post-processing was performed using LaVision DaVis 10 software while PLIF post-processing was using in-house codes.

RESULTS AND DISCUSSIONS

Outdoor dispersion

In a TBL flow, the streamwise scalar transport is dominated by the mean flow advection, while the vertical scalar transport is dominated by the turbulent diffusion mechanism. The mean concentration field is shown in figure 2(a), where the far-field plume exhibits self-similar behaviour, and the concentration vertical profiles (equation 5), plume vertical half-width

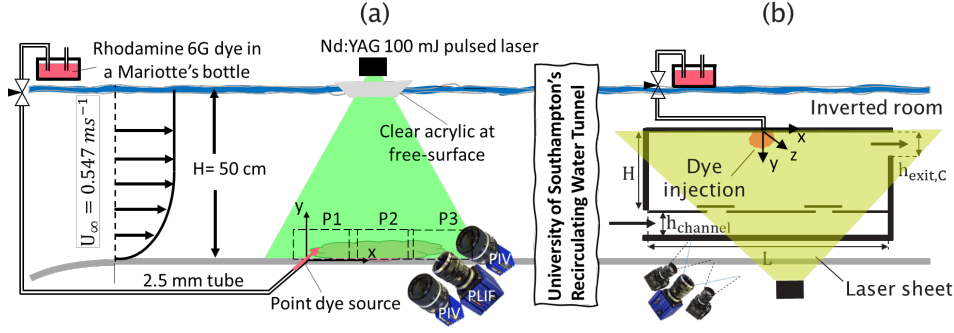


Figure 1. Schematic of the experimental setup for the (a) TBL flow and (b) the room model (mounted upside down). Not drawn to scale, both experiments were performed in separate test campaigns in the University of Southampton's water flume facility.

(equation 6) and the mean peak concentrations decay (equation 7) were observed to follow power-laws (Lim & Vanderwel, 2023):

$$\frac{\bar{C}}{C_0} = \exp \left[-\ln 2 \left(\frac{y}{\delta_y \bar{C}} \right)^{1.5} \right], \quad (5)$$

$$\delta_y \bar{C} / \delta = 0.065 \left(\frac{x - x_0}{\delta} \right)^{0.65}, \quad (6)$$

$$\frac{\bar{C}_0 U_\infty \delta^2}{Q_{dye} C_s} = 50 \left(\frac{x - x_0}{\delta} \right)^{-1.39}, \quad (7)$$

where \bar{C}_0 represents the mean peak concentration, δ represents the boundary layer thickness, x_0 represents a virtual origin shift, and Q_{dye} is the volume flow rate of the pollutant source.

These results are consistent with the literature of the scalar dispersion of a point-source in atmospheric boundary layer flow (Robins, 1978), except for the introduction of the virtual origin shift and slightly different scaling constants. In this case, the tracer dye remains trapped in the viscous sub-layer (VSL) of the smooth-wall TBL, hence a virtual origin shift of $x_0 = 1.3\delta$ was necessary. For the same reason, molecular diffusion and advection of the dye within the VSL effectively increases the source size and reduces the source strength relative to the logarithmic layer of the TBL flow. Hence, our plume is slightly wider with lower peak concentrations when compared with Robins (1978). In comparison to the Gaussian plume model, our measured power law exponents show faster plume growth and decay of the peak concentration than the traditional Gaussian plume solution which predicts the plume widths grow as $x^{0.5}$ and the peak concentration decay scales as x^{-1} . This can be attributed to non-constant turbulent diffusion coefficients.

To gain additional insights to the turbulent diffusivity, we used our measurements of the turbulent scalar fluxes and mean concentration gradient, and the first-order gradient transport model in equation 2, to calculate the different components of the turbulent diffusivity tensor based on the procedure described by Lim & Vanderwel (2023). Two-dimensional

maps of the principal D_{yy} component (fig 2b) show magnitudes that vary with wall-normal distance. Non-zero cross-diffusivity D_{yx} component were also observed (due to turbulence anisotropy), but the results (fig 2c) confirm that the contribution to the turbulent scalar fluxes is small. Overall, $K = D_{yy}$ is a good approximation for the vertical turbulent scalar fluxes, but the variation with wall-normal distance is significant which should be considered in models.

The turbulent Schmidt number relates the turbulent diffusivity coefficient, K , to the turbulent viscosity, ν_t . Using the Boussinesq's turbulent viscosity model and approximating $K = D_{yy}$, we can calculate the turbulent Schmidt number. Figure 2(d) shows Sc_t is a function of the wall-normal distance, and that the peak value of approximately 1.25 occurs at the edge of the logarithmic region of the TBL at $y/\delta = 0.2$. A peak value of above 1.0 suggests the flow structures are more effective at transporting the momentum than the scalar. This may be because the tracer scalar is only intermittently present at the plume edge (i.e. $y/\delta = 0.2$), hence the presence of a vortex may not necessarily transport the scalar, but it will always transport momentum.

Indoor dispersion

In the empty room flow, the flow is considerably more complex than a TBL flow as the flow direction varies around the room. The mean flow and scalar fields are dependent on several factors, including the ACH, ventilation design, room geometry and source position within the room. We illustrate the complexity of indoor mixing using three selected test cases, which have the exact same room geometry and ventilation parameters but with different source positions (Lim *et al.*, 2024). As shown in figure 3(a)ii, the inflow is at the top and the outflow is at the bottom right, with key dimensions of the room similar to the Nielsen benchmark model (Nielsen, 1990). The ground-level source is at either the centre (figure 3i), left (figure 3ii) or right (figure 3iii) of the room.

The mean velocity vector maps in figure 3(a)ii (flow field is similar for all three test cases) show how changing the source location leads to changes in the near-source flow fields, which have a significant influence on the shape of the mean concentration isocontour lines and scalar dispersion properties as shown in figure 3(a). This comparison shows that it is important to understand the underlying scalar transport mechanism in the near-source region, as it has the largest influence on the initial scalar dispersion patterns.

The simultaneous velocity and scalar measurements allow for direct measurements of the in-plane advective and turbulent scalar fluxes (which are shown in detail by Lim *et al.*

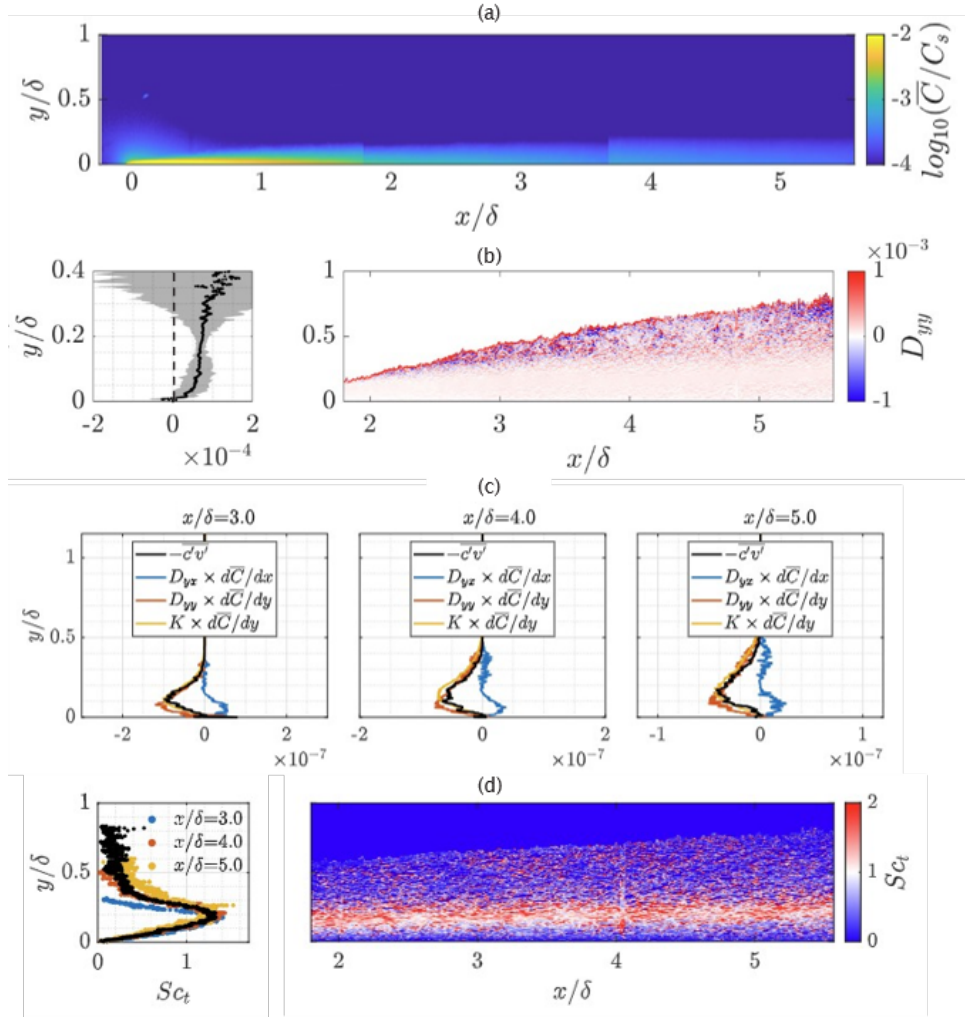


Figure 2. A continuous point-source in a TBL flow representing an outdoor scalar dispersion problem. Two-dimensional map of the (a) mean concentration of the scalar plume, (b) streamwise-median profile and map of the principal turbulent diffusivity component (D_{yy}) of the wall-normal turbulent scalar flux, (c) profiles of the contribution of the turbulent diffusivity components to the wall-normal turbulent scalar flux, and (d) the profile and map of the turbulent Schmidt number.

(2024)). Figure 3(b) shows the maps of the ratio of the magnitudes of the advective to turbulent scalar fluxes. The scalar transport mechanism in the near-source region is complex and non-linear, even when the room design and ventilation parameters are the same, and only the source location is varied.

For test cases (i) and (ii), the mean flow advection did not introduce significant directivity to the transport of the scalar or dominate the scalar transport mechanism. Rather, the scalar transport is dominated by turbulent diffusion aligned with the mean concentration gradient in the near-source region. This resulted in mean concentration isocontour lines that are relatively semicircular (fig 3(a)). For test case (iii), figure 3(b)iii shows the near-source region has advective scalar flux that are at least an order of magnitude greater than the turbulent component (values smaller than -1). The dominance of the mean flow advection introduces significant directivity to the transport of the scalar, thus resulting in mean concentration isocontour lines as shown in fig 3(a)iii.

Since the mean flow is multi-directional in the entire room domain, it makes sense to define the turbulent diffusivity with respect to the direction of the local turbulent scalar flux vector. With this definition, the turbulent scalar flux has a tangential component that is aligned with the vector, and a normal com-

ponent that is orthogonal to the vector and must therefore be zero. Hence, at every spatial location, the contributions of the concentration gradient to the turbulent scalar flux is simply:

$$-\overline{c'\mathbf{u}'}_t = D_{tt} \left. \frac{\partial \overline{C}}{\partial \mathbf{x}} \right|_t + D_{tn} \left. \frac{\partial \overline{C}}{\partial \mathbf{x}} \right|_n. \quad (8)$$

The resulting estimates of the tangential component of the turbulent diffusivity, D_{tt} , which has a dominant contribution to the turbulent scalar flux shown in equation 8, are presented in figure 3(c). Since D_{tt} dominates, the turbulent diffusivity coefficient can be estimated using $K \sim D_{tt}$. This method of focusing on the gradient transport may work well for cases (i) and (ii), which are diffusion-dominated, but works less well for case (iii) which is advection-dominated. Additionally, for both cases, this can only be estimated where there are concentration measurements near the source, but one could expect this to be representative of the room domain. The key rationale behind this is that the mean concentration decays very rapidly, by orders of magnitude, with distance from source. As such, small variations/uncertainties in the far field turbulent diffusivity would have a negligible effect on the overall

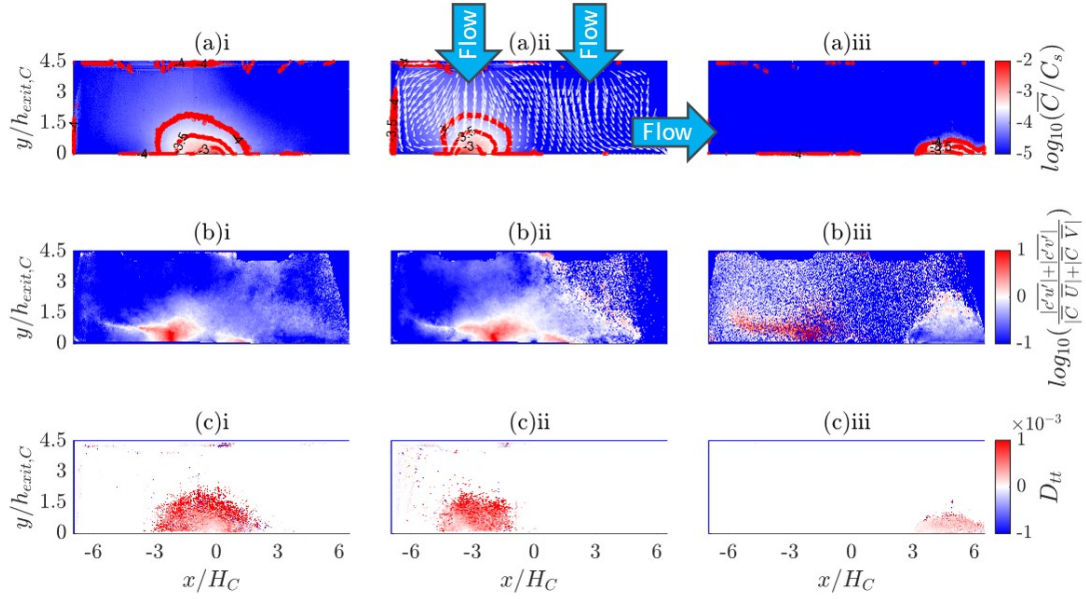


Figure 3. A continuous point-source in a 60:1 full-to-model scale empty room model representing an indoor scalar dispersion problem. (a) Mean concentration with isocontour lines, (b) ratio of the magnitudes of the advective to turbulent scalar fluxes, (c) tangential component of the turbulent diffusivity (calculated using a different method as the TBL test case) contributing to the turbulent scalar flux. Source position at $x/h_{exit,C} = (i) 0, (ii) -4.6$ and (iii) 4.6 .

scalar transport predictions. The magnitudes of the estimated turbulent diffusivities are $\mathcal{O}(10^{-3} \text{ m s}^{-2})$, and were observed to increase with distance from source and ACH.

The discussions thus far indicate a prior knowledge of the flow field is needed in order to select the most appropriate model to predict concentrations for indoor airflow applications. A caveat to the use of these models is that they are designed with specific assumptions, i.e. negligible flow advection for the Eddy Diffusion Model based on the diffusion equation. The complexity of the indoor airflow means any specific scalar dispersion model would very likely start producing inaccurate results as the scalar transport mechanism changes with the development of the scalar plume. This is exemplified by figure 3(a)iii, where the non-linear growth/decay of the vertical height of the plume cannot be accurately captured with any existing models.

Discussions on turbulent diffusivity

A practical aspect of scalar dispersion models is the reliance on an appropriate value of the turbulent (eddy) diffusivity coefficient. Nonetheless, estimating this value may not be straightforward, and it must be made clear whether this parameter encompasses turbulent transport only (Vanderwel & Tavoularis, 2014; Lim & Vanderwel, 2023; Lim *et al.*, 2024) or both advective and turbulent scalar transport (Foat *et al.*, 2020; Cheng *et al.*, 2011; Nicas *et al.*, 2009). This is dependent on whether the scalar dispersion problem is modelled using an advection-diffusion equation framework or the diffusion equation framework, as discussed previously in the introduction.

Estimates of the eddy diffusion coefficients, obtained by matching diffusion-based model predictions to real-world measurements, scaled experiments or high-fidelity CFD data, would inherently combine the scalar transport mechanisms associated with both eddy diffusion (due to small-scale turbulence) and mean advection (due to mean flow patterns or large-

scale flow structure). Strictly speaking, diffusion-based models do not actually ignore the contributions of the mean flow advection. Instead, they assume the presence of any large-scale flow structures or the mean flow have an isotropic and homogeneous effect on the scalar transport. This would mean a disparity in the eddy diffusion coefficients obtained based on the advection-diffusion equation approach in comparison to the diffusion-based equations. In our recent study (Lim *et al.*, 2024), we showed that our experimental measurements of the eddy diffusion coefficients, based on the gradient transport model and advection-diffusion equation framework, are lower than the eddy diffusion coefficients obtained based on the diffusion based equation (Cheng *et al.*, 2011; Shao *et al.*, 2017) for similar room flow conditions.

Currently, there is no discrimination on what the term ‘eddy diffusivity’ represents. However, it is important to use different ‘eddy diffusion coefficient’ terminologies, depending on whether it is based on the advection-diffusion or the diffusion framework. Henceforth, we recommend to use the term ‘eddy diffusion coefficient’ (K) for methods based on the advection-diffusion equation approach (Lim & Vanderwel, 2023; Vanderwel & Tavoularis, 2014) and the term ‘total eddy diffusion coefficient’ (K_{total}) for methods based on the diffusion equation approach (Foat *et al.*, 2020).

One final point on turbulent diffusivity models is the effect of assuming isotropic turbulence, and approximating the turbulent diffusivity tensor to a single coefficient. In outdoor flows, approximating $K \sim D_{yy}$ and neglecting the contributions of D_{yx} did not introduce significant uncertainties to the vertical scalar transport as shown in figure 2(c) (discussed in detail in Lim & Vanderwel (2023)). However, in indoor airflows, flow turbulence can be highly anisotropic, and the contribution of the orthogonal concentration gradient to the principal turbulent scalar flux may not be insignificant. Lim *et al.* (2024) experimentally measured the turbulent scalar fluxes and

mean concentration gradients in equation 2, and showed that although the principal component of the turbulent diffusivity D_{tt} is dominant (fig 3(d)), by approximating D_{ij} to a single turbulent diffusion coefficient (i.e. $K \sim D_{tt}$) and neglecting the contributions from D_{nn} , this would introduce an average error of around 18% for the test cases that were studied.

CONCLUSIONS

Both outdoor and indoor predictions of turbulent scalar transport rely on the application of turbulent diffusivity models; however, with different assumptions. The treatment of the advective flux is particularly complex in indoor flows, which has implications on the choice of appropriate scalar dispersion models and the associated uncertainties in predicted concentrations. In both cases, the turbulent diffusivities measured are observed to be anisotropic and non-homogeneous, which can lead to further errors in the predictions of these models.

Another important aspect of turbulent diffusivity models is that there is currently widespread use of the same ‘eddy diffusion’ terminology in the literature, without discrimination on whether the scalar transport model is based on the advection-diffusion or the diffusion equation framework. We have discussed the benefits and suitability of both approaches and recommend air quality practitioners ensure that their chosen framework is properly specified to avoid using inappropriate diffusivity coefficients for dispersion modelling.

Future work

There are a few outstanding research questions that we are keen to address in future work. Firstly, the indoor-outdoor pollutant flux has not been considered in this study. With rapid global urbanisation the defining trend of the 21st century, the number of cities and megacities are projected to continue increasing all over the world. This changes the sources/sinks and dispersion properties of air pollutants in the built environment. The indoor-outdoor pollutant flux has a strong influence on air quality and is an extra layer of complexity that needs to be considered.

Secondly, pollutant monitors are typically point measurement stations/devices. Sparse pollutant concentration monitors may work well for outdoor applications where there is often existing meteorological data to inform dominant wind patterns and the placement of these monitors. For indoor airflows however, the strong dependence of the mean concentration field on the boundary conditions means selecting the monitor location can be challenging, and multiple (usually wall-mounted) low-cost monitors may be needed to provide representative indoor air quality estimates.

Finally, we have not considered the influence of human activities, which can contribute to anthropogenic sources of pollutants or the introduction of turbulence for indoor scalar mixing problems, heterogeneous roughness of city layouts for outdoor pollutant transport, the atmospheric chemistry of primary and secondary (i.e. reactive) pollutants, dry and wet deposition effects, etc. Clearly, the topic of air quality is very diverse, and would benefit from multi-disciplinary approaches to the research problem.

In this TSFP presentation, we have presented a high-level overview of the lessons learned from CV’s UKRI Future Leader’s Fellowship and HDL’s Royal Academy of Engineering Fellowship on outdoor and indoor dispersion, respectively, the funding from which we gratefully acknowledge.

REFERENCES

- Calder, K.L. 1965 On the equation of atmospheric diffusion. *Quarterly Journal of the Royal Meteorological Society* **91** (390), 514–517.
- Carruthers, D.J., Edmunds, H.A., Lester, A.E., McHugh, C.A. & Singles, R.J. 2000 Use and validation of adms-urban in contrasting urban and industrial locations. *International Journal of Environment and Pollution* **14** (1-6), 364–374.
- Cheng, K.C., Acevedo-Bolton, V., Jiang, R.T., Klepeis, N.E., Ott, W.R., Fringer, O.B. & Hildemann, L.M. 2011 Modeling exposure close to air pollution sources in naturally ventilated residences: Association of turbulent diffusion coefficient with air change rate. *Environmental Science & Technology* **45** (9), 4016–4022.
- Cimorelli, A.J., Perry, S.G., Venkatram, A., Weil, J.C., Paine, R.J., Wilson, R.B., Lee, R.F., Peters, W.D. & Brode, R.W. 2005 Aermid: A dispersion model for industrial source applications. part i: General model formulation and boundary layer characterization. *Journal of Applied Meteorology and Climatology* **44** (5), 682–693.
- Foat, T.G., Drodge, J., Nally, J. & Parker, S.T. 2020 A relationship for the diffusion coefficient in eddy diffusion based indoor dispersion modelling. *Building and Environment* **169**, 106591.
- van Hooff, T., Blocken, B., Gousseau, P. & van Heijst, G.J.F. 2014 Counter-gradient diffusion in a slot-ventilated enclosure assessed by les and rans. *Computers & Fluids* **96**, 63–75.
- Lim, H.D., Foat, T.G., Parker, S.T. & Vanderwel, C. 2024 Experimental investigation of scalar dispersion in indoor spaces. *Building and Environment* **250**, 111167.
- Lim, H.D. & Vanderwel, C. 2023 Turbulent dispersion of a passive scalar in a smooth-wall turbulent boundary layer. *Journal of Fluid Mechanics* **969**, A26.
- Mingotti, N., Wood, R., Noakes, C.J. & Woods, A.W. 2020 The mixing of airborne contaminants by the repeated passage of people along a corridor. *Journal of Fluid Mechanics* **903**, A52.
- Nicas, M., Keil, C., Simmons, C. & Anthony, T. 2009 Turbulent eddy diffusion models. *Mathematical Models for Estimating Occupational Exposure to Chemicals* pp. 53–65.
- Nielsen, P.V. 1990 *Specification of a Two-Dimensional Test Case: (IEA). Gul Serie 8*. Institut for Bygningsteknik, Aalborg Universitet, international Energy Agency, Energy Conservation in Buildings and Community Systems, Annex 20: Air Flow Pattern within Buildings PDF for print: 22 pp.
- Robins, A.G. 1978 Plume dispersion from ground level sources in simulated atmospheric boundary layers. *Atmospheric Environment (1967)* **12** (5), 1033–1044.
- Shao, Y., Ramachandran, S., Arnold, S. & Ramachandran, G. 2017 Turbulent eddy diffusion models in exposure assessment-determination of the eddy diffusion coefficient. *Journal of Occupational and Environmental Hygiene* **14** (3), 195–206.
- Stockie, J.M. 2011 The mathematics of atmospheric dispersion modeling. *Siam Review* **53** (2), 349–372.
- Tavoularis, S. & Corrsin, S. 1985 Effects of shear on the turbulent diffusivity tensor. *International Journal of Heat and Mass Transfer* **28** (1), 265–276.
- Vanderwel, C. & Tavoularis, S. 2014 Measurements of turbulent diffusion in uniformly sheared flow. *Journal of Fluid Mechanics* **754**, 488–514.